

MHSCNet: A Multimodal Hierarchical Shot-aware Convolutional Network for Video Summarization

Wujiang Xu*

MYBank, Ant Group; School of Software, Xi'an Jiao-tong
University
Xi'an, China
xuwujiang.xwj@mybank.cn; xjtuwujiangxu@stu.xjtu.edu.cn

Shaoshuai Li; Qiong Xu Ma; Yunan Zhao

Sheng Guo
Xiaobo Guo[†]
Bing Han
MYBank, Ant Group
Hangzhou, China
{lishaoshuai.lss, qiongqu.mqx, yunan.zya}@mybank.cn
{guosheng.guosheng, jeflittleguo.gxb, hanbing.hanbing}@mybank.cn

Junchi Yan

Department of Computer Science and Engineering,
Shanghai Jiao Tong University
Shanghai, China
yanjunchi@cs.sjtu.edu.cn

Yifei Xu

School of Software, Xi'an Jiao-tong University
Xi'an, China
belonxu_1@xjtu.edu.cn

ABSTRACT

Video summarization intends to produce a concise video summary by effectively capturing and combining the most informative parts of the whole content. Existing approaches for video summarization regard the task as a frame-wise keyframe selection problem and generally construct the frame-wise representation by combining the long-range temporal dependency with the unimodal or bimodal information. However, the optimal video summaries need to reflect the most valuable keyframe with its own information, and one with semantic power of the whole content. Thus, it is critical to construct a more powerful and robust frame-wise representation and predict the frame-level importance score in a fair and comprehensive manner. To tackle the above issues, we propose a multimodal hierarchical shot-aware convolutional network, denoted as MHSCNet, to enhance the frame-wise representation via combining the comprehensive available multimodal information. Specifically, we design a hierarchical ShotConv network to incorporate the adaptive shot-aware frame-level representation by considering the short-range and long-range temporal dependency. Based on the learned shot-aware representations, MHSCNet can predict the frame-level importance score in the local and global view of the video. Extensive experiments on two standard video summarization datasets demonstrate that our proposed method consistently outperforms state-of-the-art baselines. Source code will be made publicly available.

CCS CONCEPTS

• Computing methodologies → Video summarization.

KEYWORDS

Shot-aware Representation, Multimodal information, Video Summarization

1 INTRODUCTION

The explosive ubiquity of digital photography brings a phenomenal surge in videos captured every day. Confronted with the enormous amount of video data, apparently, it is impractical for end-user to browse the videos completely to understand the content. To address this issue, video summarization has gained increasing attention to figure out how to browse, manage and retrieve videos efficiently [26, 48, 51]. The objective of video summarization is to create a short synopsis that preserves the most important and relevant content of the original video with minimal redundancy [42, 53, 59].

Typically, the most recent video summarizers follow the three steps: 1) video segmentation, 2) importance score prediction, and 3) key shot selection. Regarding video segmentation, KTS (Kernel Temporal Segmentation) is widely used to segment the coherent frame sequence into several shots [38]. As for key shot selection, it is tackled by 0-1 knapsack algorithm to generate a key-shot based summary. The most challenging step is importance score prediction, which is designed to highlight the most important parts according to the predicted scores for the video content. Previous works have devised different approaches to cope with this key challenge. They can be roughly categorized into unsupervised [13, 57], weakly-supervised [17, 32] and supervised methods [7, 51]. Recent unsupervised methods attempt to reconstruct the video based on the key-shot summary generated by the frames' importance score [8, 26]. Also, the diversity and sparsity of output summary [33–35, 41, 48] are introduced as repelling regularizers in the training loss. For the weakly-supervised methods, the video-level meta-data, such as video titles [32, 50], web priors [1, 2] and video categories [38], work as the auxiliary information to put additional constraints for video summarizers. Although unsupervised and weakly-supervised methods have reached promising performance, the supervised methods always perform better benefiting from the manually annotated dataset.

To manipulate video frames for supervised video summarizers, it is desirable to handle temporal dependency among video frames effectively. To achieve this, recent efforts exploited LSTM units [52,

*Work done during an internship at MYBank, Ant Group.

[†]Contact Author.

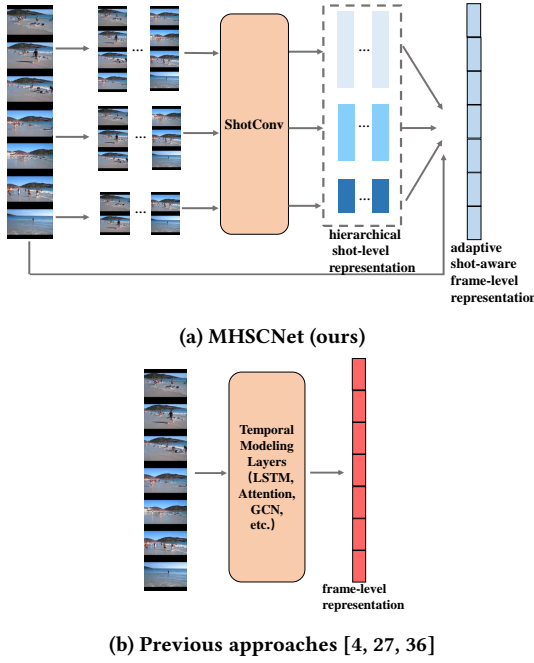


Figure 1: (a) The proposed MHSCNet builds adaptive shot-aware frame-level representation by modeling the frame-to-frame interaction and incorporating the hierarchical shot-level representation into the frame-level representation. (b) In contrast, previous approaches [4, 27, 36] utilize different temporal modeling layers (LSTM, Attention, GCN, etc.) to produce the frame-level representation containing the long-range temporal dependency.

53, 55] to capture long-range temporal dependency among video frames. Besides, some methods [4, 8, 24] resorted to the attention mechanism to propagate the temporal dependency information in the frame level. To better perform relationship reasoning among the frames, Park et al. [36] introduced a recursive graph structure and achieved the state-of-the-art performance. Apart from the unimodal approaches, some bimodal methods [21, 31] extract important frame by fusing the textual as well as video metadata and remarkable performance could be achieved. Recently, the work [27] proposed a language-guided bimodal transformer via fusing information across the video and language modalities.

Despite the promising success, existing video summarization methods still encounter two major challenges. First, *how to construct a more powerful and robust frame-wise representation for video summarization?* Essentially, most of the above methods [27, 36, 59] only adopted visual cues or textual video metadata to construct the frame-wise representation. However, almost all videos include an audio track, which could provide vital complementary information for the frame-wise representation. For instance, in a scene when a man has a conversation with a woman, we only see the two people sit aside but the audio helps us to understand the dialogue content. Meanwhile, a caption usually highlights the subject of a video, which can help us to select the relevant shots. Therefore, it is critical

for a model to consider the multimodal information to construct a more powerful and robust frame-wise representation for video summarization. Second, *how to predict the frame-level importance score in a fair and comprehensive manner?* The previous approaches [4, 27, 36] mainly focused on extracting the long-range temporal dependencies to predict the importance score of the frames from the global view, which inevitably overlooks the important frames within the local shot. As we know, video temporal structures are intrinsically layered, i.e., a video is composed of shots, and a shot is composed of several frames. Suppose a shot of blowing candles consists of three sample frames which represent taking out the lighter, lighting candles, and blowing out candles, respectively. Considering the visual coherence of the key-shot summary, the importance scores of the three consecutive frames will influence each other internally. Thus, lacking in modeling the frame-to-frame interaction within the shot the previous methods unfairly evaluate the frame importance score and generate inaccurate summary results.

To address the above challenges, we present a multimodal hierarchical shot-aware convolutional network, referred to **MHSCNet**, to exhaustively exploit the available modality information of the video to enhance the frame representation, and model the frame-to-frame interactions explicitly within the shot to pay attention to the important frames both in the local and global view. The shot-aware network means that the inner operation among the network is defined at the shot level. As illustrated in Fig. 2, it first encodes the multimodal inputs individually with pre-trained models to generate separate representations and then aggregates them hierarchically to explore the semantic relations. Subsequently, to answer the first challenge, MHSCNet fully exploits the modality information including the audio and the caption of the video to construct a robust and informative frame-wise representation. Moreover, to answer the second challenge, we design a hierarchical shot-aware convolutional network with the progressive cross-shot padding mechanism to generate an adaptive shot-aware representation, which contains both short-range and long-range temporal dependency. As illustrated in Fig. 1a, MHSCNet builds the adaptive shot-aware frame-level representation which perceives shot-level information by modeling the frame-to-frame interaction in the hierarchical shot-level and incorporating the shot-level representation into the frame-wise representation. In contrast, previous approaches [4, 27, 36] generally investigated the long-range temporal dependency to construct the frame-wise representation by different temporal modeling layers (LSTM, Attention, GCN, etc.) leading to ignoring the important frames in the local view. Benefiting from the adaptive shot-aware representation, our MHSCNet can evaluate the frame-level importance score in a fair and comprehensive view.

The contributions of this work are summarized as follows:

- We propose a multimodal framework to fully explore the semantic relations among the modalities and construct a powerful and robust frame-wise representation for video summarization.
- We design a hierarchical ShotConv network with the cross-shot padding mechanism to produce the adaptive shot-aware representation, which offers a fair and comprehensive view to predict the importance scores of the frames. Due to the hierarchical design, the shot-aware representation containing both the short-range and long-range temporal dependency.

- The experiment results indicate that our proposed method outperforms existing state-of-the-art methods on two benchmarks. Besides, we also conduct extensive ablation studies and detailed analyses to verify the effectiveness of our method. Our code will be available for further comparison.

2 RELATED WORK

Given an input video, video summarization intends to generate a shortened version that contains the most important information, resulting in outputs such as video synopses [39], time-lapses [12, 18, 37], montages [14, 45], or storyboards [20, 23]. Early works in video summarization primarily relied on hand-crafted heuristics [16, 17, 20, 25, 28, 34], including importance, representativeness and diversity to select representative frames to produce a summary video. Nowadays, deep neural networks for video summarization have achieved great success. Focusing on the utilized modality information, we can briefly outline two categories of video summarization methods: 1) unimodal methods, 2) bimodal methods.

2.1 Unimodal Video Summarization

In the past, most researchers [52, 53, 55] utilized the unimodal visual information to construct the frame representation and resorted to the recurrent neural network like LSTM to exploit the long-range temporal dependency. Although LSTM-based approaches have been applied to video data, recurrent operations are sequential, limiting the processing all the frames simultaneously. To tackle this problem, Fajtl et al. [4] proposed a self-attention mechanism based network for video summarization which executes the entire sequence to sequence transformation. He et al. [8] built their framework upon a generative adversarial network which is composed of the self-attention module. To capture multiple concepts, Liu et al. [24] introduced the multi-head attention mechanism. Rochan et al. [42] constructed a fully convolutional sequence model and formulated video summarization as a sequence labeling problem. Different from these methods, Zhu et al. [59] proposed a Detect-to-Summarize network which predicted the corresponding importance scores and temporal locations of segments via defining video summarization problem as a temporal interest detection process. Park et al. [36] utilized a recursive graph to perform relationship reasoning among frames. However, these unimodal approaches only adopt the visual modality information, leading to the insufficient frame representation.

2.2 Bimodal Video Summarization

Unlike unimodal video summarization methods, existing bimodal video summarization methods fused additional audio or caption information to enhance the frame representation. Zhou et al. [58] combined the category-related information with the frame feature. Huang et al. [10] designed a bimodal framework consisting of a contextualized video summary controller and bimodal attention mechanisms to explore the power of text modality. Yuan et al. [49] constructed a latent subspace to find the meaningful frame-level feature with side semantic information. Zhao et al. [54] developed an AudioVisual Recurrent Network to jointly exploit the audio and visual information for the video summarization. Recently,

Narasimhan et al. [27] proposed a language-guided bimodal transformer for both generic and query-focused video summarization. While these methods resort to the bimodal information and the long-range temporal dependency, ignoring the potential of fully incorporating available multimodal information and the short-range temporal dependency they miss the key-shot summary. To construct a powerful and robust representation and fully consider the locally-global side information, we build our MHSCNet with both the audio and the caption modal information.

3 METHODOLOGY

3.1 Motivation and Approach Overview

Manual video summarization generally extracts key information by means of video segmentation and subsequent ordinal or unordered shot-shot pairwise significance ordering [6, 44], which indicates that the frames within the same shot will interact with each other and all determined to be chosen or not for the key-frame summary. Meanwhile, the human annotator will consider the subject of the video via the audio and the textual information to judge the relevance between the frame and the video. The aforementioned methods mainly consider the long-range temporal dependency to enhance the frame-level representation via little additional modality information, ignoring the mutual relations between the contiguous frames within the same shot. Motivated by the manual annotation procedure, we propose a hierarchical ShotConv network that takes the aggregated multimodal feature as input and outputs the adaptive shot-aware representation preserving the short-range temporal dependency within the shot and the long-range temporal dependency across the shot via the proposed cross-shot padding mechanism. During the inference stage, it is hard to set the fixed length of the shot due to the variability of the shot segmentation. To make our network adaptive to the variable video length, we fix the different shot lengths for our sub-ShotConv modules. Overall, our framework mainly has two modules as shown in Fig. 2, where the first module is multimodal feature fusion, and the second module is a hierarchical ShotConv network. During the inference, the video is firstly segmented to the several shots by the Kernel Temporal Segmentation algorithm [38]. Then, the importance scores of the frames are predicted by our MHSCNet. Finally, the 0-1 knapsack algorithm is utilized to generate a key-shot based summary.

3.2 Feature Extraction

Given a video V as a sequence of T frames, we first employ CNN (e.g. GoogLeNet) without the last three layers to extract feature $F_V = [f_{v_1}, \dots, f_{v_i}, \dots, f_{v_T}] \in \mathbb{R}^{T \times N}$. For audio information $F_A = [f_{a_1}, \dots, f_{a_i}, \dots, f_{a_T}] \in \mathbb{R}^{T \times M}$, the VGGish [9] pre-trained on Audioset is adopted for audio feature extraction and the sampling frequency is set for keeping the same sequence length with the frame feature. To capture generic caption information, we use the Bi-Modal Transformer [11] to generate dense video captions for the whole video. We use the CLIP [40] model to encode caption vector $F_C \in \mathbb{R}^{1 \times N}$ and average pooling is used to balance multiple sentences.

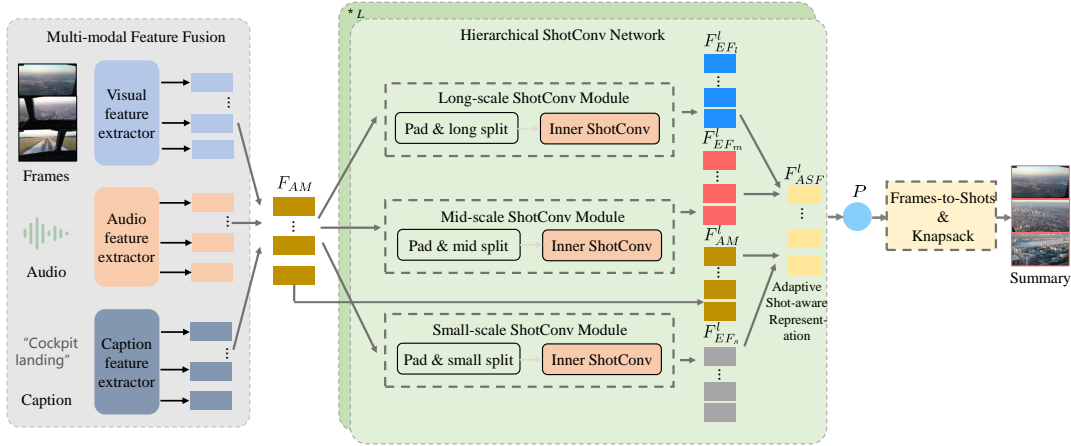


Figure 2: Overview of our multimodal hierarchical shot-aware convolutional network (MHSCNet), consisting of the multi-modal feature fusion and a hierarchical ShotConv network. In inference, the summary of the original video is generated by transforming frame scores to shot scores and a 0-1 knapsack algorithm is used to select high-scoring shots in the limited summary length.

3.3 Multimodal Feature Fusion

3.3.1 Audio Feature Fusion. Firstly we fuse the image feature with the audio feature to explore the semantic relations. For the i -th frame, we project the audio vector f_{a_i} to the same embedding space with the image feature F_V by a trainable matrix W_{audio} like Eq. 1.

$$f_{va_i} = f_{v_i} + f_{a_i}W_{audio} + b_{audio} \quad (1)$$

where $W_{audio} \in \mathbb{R}^{M \times N}$, $b_{audio} \in \mathbb{R}^N$ are the trainable matrices and the trainable bias, respectively.

3.3.2 Caption Feature Fusion. After fusing the audio information, we also incorporate prior knowledge into the frame feature. To this end, we employ the multi-head attention mechanism to fuse the caption feature F_C . We regard the caption feature F_C as both the Key and the Value and the enhanced local feature F_{VA} as the Query. Therefore, the aggregated multimodal frame-level feature F_{AM} can be calculated as follows:

$$F_{AM} = \text{Concat}(\text{head}_1, \dots, \text{head}_h)W^O \quad (2)$$

$$\text{head}_j = \text{Attention}(QW_j^Q, KW_j^K, VW_j^V) \quad (3)$$

$$\text{Attention}(Q, K, V) = \text{softmax}\left(\frac{QK^T}{\sqrt{d_k}}\right)V \quad (4)$$

where $W^O \in \mathbb{R}^{N \times N}$, $W_j^Q \in \mathbb{R}^{N \times d_k}$, $W_j^K \in \mathbb{R}^{N \times d_k}$ and $W_j^V \in \mathbb{R}^{N \times d_k}$ are trainable matrices, $d_k = N/h$ and h is the number of attention heads.

3.4 Hierarchical ShotConv Network

3.4.1 Cross-shot Padding & Split. As shown in Fig. 3, we firstly pad the specified number of frames in the boundary of the each shot to maintain the consistent temporal information. Given a padding ratio η and the shot number S , $\eta \times \lfloor \frac{T}{S} \rfloor$ frames from the end of the $(S-1)$ -th shot will be padded at the start of the S -th shot. For the consistency, we pad the parts of frames from the last shot to the start of the first shot. Then a 1×1 convolution is utilized to increase

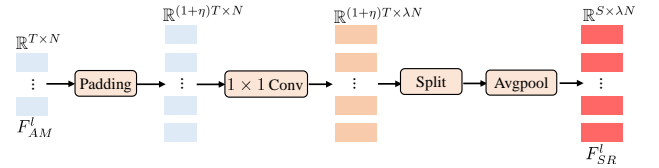


Figure 3: The cross-shot padding & split module.

the channel of the frame from N to λN and the frame-level feature $F_{CP}^l = [f_{cp_1}^l, \dots, f_{cp_i}^l, \dots, f_{cp_{(1+\eta)T}}^l] \in \mathbb{R}^{(1+\eta)T \times \lambda N}$ in the l -th layer could be obtained via the cross-shot padding mechanism. Then, we reshape the dimension from $(1+\eta)T \times \lambda N$ to $S \times (D_S \cdot \lambda N)$, where $D_S = \lfloor \frac{(1+\eta)T}{S} \rfloor$ and $\lfloor \cdot \rfloor$ is the round down function to transform the frame-level representation to the inflated shot-level representation F_{ISR}^l . Specially, the s -th shot contains the features of inside frames as follows:

$$F_{ISR_s}^l = \{f_{cp_k}^l : k = (s-1)D_S + 1, \dots, sD_S, sD_S + 1\} \quad (5)$$

Lastly, an average pooling operator will be used on the dimension D_S of the frame number to obtain the concentrated shot-level representation $F_{SR}^l \in \mathbb{R}^{S \times \lambda N}$. To make our network adaptive to the video length, we propose three scales cross-shot padding, and the shot number S will be set to S_l, S_m, S_s for the long scale, middle scale, and short scale to generate the corresponding representation $F_{SR_l}^l, F_{SR_m}^l$ and $F_{SR_s}^l$.

3.4.2 Inner ShotConv Module. As shown in Fig. 4, we propose an inner shot convolution module to model the frame interaction within the shot. The inner shot convolution module is composed of four convolution operators with different kernel sizes and other postprocessing modules. The strides of the four convolution operators are set to 4. The 5×5 and 7×7 convolution operators are implemented by the dilated convolution [47]. We firstly perform

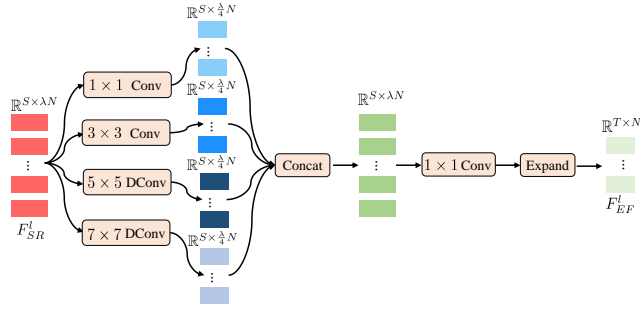


Figure 4: The inner shot convolution module.

these four convolution operators on the shot-level feature F_{SR}^l . Then we will concatenate them in the channel dimension and feed it to a 1×1 convolution layer to reduce the channel dimension from λN to N . Each shot-level representation will be assigned to the frames in the same shot to get the enhanced frame-level representation F_{EF}^l via the expand operation. For the three scales ShotConv modules, the enhanced frame-level representation $F_{EF_l}^l$, $F_{EF_m}^l$ and $F_{EF_s}^l$ are generated for the long scale, middle scale and short scale, respectively. As shown in Fig. 4, the adaptive shot-aware representation $F_{ASF}^l \in \mathbb{R}^{T \times N}$ is obtained after the multi-scale ShotConv modules by Eq. 6.

$$F_{ASF}^l = F_{EF_l}^l + F_{EF_m}^l + F_{EF_s}^l + F_{AM}^l \quad (6)$$

where F_{AM}^l will be replaced by F_{ASF}^{l-1} except the first layer. We stack L layers of the hierarchical ShotConv network and the output from each layer will be the input of the next layer.

3.4.3 Implicit Global Information Propagation. In each layer of the ShotConv network, cross-shot padding will propagate information between two adjacent shots. Benefitting from this cross-shot padding mechanism, the frames in the local shot will learn the information from the other adjacent shot. After several stacked ShotConv networks, the frames in the local shot can learn the information from the whole video since the global information will be passed in the deeper layers. Formally, the global information will be passed in a local shot when the number of stacked layers and the shot number meet the criteria as illustrated in Eq. 7.

$$L + 1 \geq S_l \quad (7)$$

where L is the number of the stacked hierarchical ShotConv network and S_l is the shot number of the long scale ShotConv module.

3.5 Loss Function

We apply the focal loss [22] for keyframe classification, which deals with the imbalance between the number of keyframes and the number of background frames. Moreover, the difference of the hard/easy sample will be highlighted. The loss is defined by:

$$\mathcal{L} = -\frac{1}{T} \sum_{t=1}^T [\alpha y_t (1 - p_t)^\gamma \log(p_t) + (1 - \alpha)(1 - y_t) p_t^\gamma \log(1 - p_t)] \quad (8)$$

where y_t is the groundtruth label of the t -th frame. α and γ are the re-weighting factor. p_t is the prediction of our proposed model.

4 EXPERIMENTS

4.1 Experiment Setup

Implementation Details. To ensure fair comparisons with prior works [36, 42, 59], we use the ImageNet-pretrained GoogleNet [46] for frame feature extraction, where the 1024-d feature are extracted after the 'pool5' layer. The dimension of the audio feature extracted by the pre-trained VGGish [9] is 128. For the generated multiple captions by the BMT [11], we use CLIP [40] to encode them and concatenate the embedding in the channel dimension. The dimension of the first fully-connected layer is 128. The number of multi-head in the caption feature fusion module is set to 32. We set $S_l = 5$, $S_m = 10$, $S_s = 15$, $\eta = 0.05$, $L = 4$ and $\lambda = 8$ in Sec. 3.4. α and γ in the focal loss are set to 0.25 and 2. All the experiment results are reported in 5-fold cross validation. Adam works as the optimizer with an initial learning rate of $1e^{-4}$, and a weight decay of $1e^{-5}$. All the comparative models are trained for 100 epochs in total and tested on the same machine, which has a single NVIDIA GeForce Titan V GPU and Intel Core i7-8700K CPU.

Datasets. We evaluate the performance of our approach on two standard video summarization datasets: SumMe [6] and TVSum [44]. SumMe dataset contains 25 personal videos obtained from YouTube which covers multiple categories such as cooking and sports. Each video ranges from 1 to 6 minutes and each reference summary is generated by 15 to 18 persons. TVSum dataset consists of 50 YouTube videos which contain 10 categories including changing vehicle tire, parade, and dog show. The video lengths of TVSum which are a little longer than SumMe vary from 2 to 10 minutes. Beside, two additional datasets including the YouTube [3] and the OVP [3] are used to augment the training data. The OVP dataset contains 50 video sequences and the YouTube dataset consists of 40 video sequences. In detail, we follow [52] to sample the frame at 2 fps to handle temporal redundancy and reduce computation. The pre-processed datasets including the data splits can be found in the URLs¹ provided by the previous researchers [56, 59].

Data configuration. We apply three data configurations adopted in [42, 51, 57] within our experiments including standard data setting, augmented data setting, and transfer data setting.

Standard: In standard data setting, the training and testing data come from the same benchmark. Typically, we randomly select 80% of videos for training and validation while 20% of videos for testing. The results of the selected dataset split stay the same with previous works [52, 59].

Augment: In the augment data setting, the videos of YouTube and OVP datasets are utilized to augment the training data. Thanks to more abundant training data, the model performance will be improved in this data setting [42, 53].

Transfer: In the transfer data setting, the videos of three datasets will be used as the training data and the videos of one another dataset (e.g. SumMe or TVSum) will be used as the testing data.

For reliable comparisons, all the experiments are conducted five times and the average performance is reported in our paper. We report the results at F-score in all of the settings. Experiments at other metrics and the ablation study are all conducted in a standard supervision manner.

¹<https://github.com/li-plus/DSNet>; <https://github.com/KaiyangZhou/pytorch-vsum-reinforce>

Evaluation Criteria. Following the previous works [7, 30, 44], F-score is used to evaluate the agreement between the generated summary and the user summary(GT). Let Y and Y^* be the ground-truth summary and the generated keyshot summary, respectively. The precision and the recall are calculated as follows:

$$P = \frac{\text{length}(Y \cap Y^*)}{\text{length}(Y^*)}, R = \frac{\text{length}(Y \cap Y^*)}{\text{length}(Y)} \quad (9)$$

We compute the F-score to evaluate the quality of the generated keyshot summary based on the precision and the recall like Eq. 10.

$$F = \frac{2 \times P \times R}{P + R} \quad (10)$$

For datasets with multiple human annotations, we follow standard approaches described in [7, 26, 44, 52] to calculate the metrics for the videos. Similar to [57, 59], we evaluate the diversity score of the generated summary on the SumMe and TVSum datasets. In recent work, Otani et al. [29] showed that randomly generated summaries achieve a similar F-score with the state-of-the-art methods. Therefore, two rank correlation coefficients, precisely Kendall's τ [15] and Spearman's ρ [60] are also used to evaluate the effectiveness of our model.

4.2 Comparisons to the State-of-the-Arts

Quantitative comparison. To validate the effectiveness of our proposed method on the video summarization problem, we quantitatively compare our proposed model against other state-of-the-art methods including unimodal methods and bimodal methods on the SumMe and TVSum datasets. As reported in Table 1, our MHSCNet achieves a significant improvement ranging from 3.7% to 13.6% on F-score in the standard data setting compared to the state-of-the-art methods equipped with the same backbone network.

The unimodal methods can be roughly classified into four categories: 1) LSTM-based methods(dppLSTM [52], SUM-GAN [26], DR-DSN [57]); 2) Attention-based methods(ACGAN [8], VASNet [4], MC-VSA [24], DASN [5]); 3) Convolution-based methods(SUM-FCN [42], SUM-DeepLab [42]); 4) Other methods(DSNet-AB [59], DSNet-AF [59], SumGraph [36]). Random summary [29] is generated by means of random importance scores and KTS video segmentation algorithm [38]. Specifically, existing LSTM-based methods achieve better performance on the TVSum dataset and relatively worse performance on the SumMe dataset against other methods. Such poorly-balanced performance indicates that the long-range dependence feature extracted by LSTM-based networks cannot work on the SumMe dataset and the relation across the shots is weak on the SumMe dataset. Different from the LSTM-based methods, attention-based methods perform slightly better on the SumMe dataset. Benefitting from the designed structure, the attention-based methods can implicitly capture the local information within the shot. Similarly, convolution-based methods extract the short-range temporal dependency within the shot implicitly. Moreover, DSNet formulate video summarization as an interest detection problem. The proposed center-ness score loss leads the model to learn more information within the shot. Besides, SumGraph perform better than DSNet by explicitly modeling relationships among the frames using a recursive graph. Benefitting from the multimodal information and adaptive shot-aware representation, our MHSCNet

outperforms SumGraph by a wide margin. Besides the unimodal methods, the bimodal methods equipped with the same backbone (GoogleNet) drop the performance ranging from 3.7% to 12.3% in the standard data setting compared to our proposed MHSCNet because they overlook the inner-shot information and involve extra modality information excessively.

We also analyze the diversity to verify the generated summary by MHSCNet contains more diverse key-frames. As shown in Table 2, our method MHSCNet outperforms LSTM-based methods (dppLSTM [52] and DR-DSN [57]) and other methods (DSNet-AF [59] and DSNet-AB [59]) with improvement ranging from 5.3% to 14.1%.

As Otani et al. [29] has indicated that random summary could achieve similar results compared to the state-of-the-art methods due to the limitation of the video segmentation methods and the 0-1 knapsack algorithm. Therefore, we directly measure importance scores using two rank correlation coefficients including Kendall's τ and Spearman's ρ between the predicted ordering and the human annotators' ordering. The results of quantitative comparisons are displayed in Table 3. We observe that MHSCNet surpasses the state-of-the-art methods including the unimodal methods and the bimodal methods with improvements of 3.8% and 7.8% at least on Kendall's τ and Spearman's ρ , respectively. From the result of human annotators, we infer that our model possesses comparable discrimination ability with the single experienced annotator. In summary, as MHSCNet jointly exploits the relations among the frames within the shot and across the shots explicitly, more discriminated and robust information could be captured. Various experiment results verify the superiority of our method.

Qualitative Analysis. We present the groundtruth importance scores and the selected frames generated by DSNet [59] and MHSCNet in Fig. 5. To visualize the summaries, we randomly sample five frames from the selected key shot summaries. The gray bars represent the groundtruth importance scores and the red bars represent the selected summary. Compared to DSNet-AF [59], the summaries produced by MHSCNet are more diverse and informative. Moreover, the generated summary captures most of the peak regions of the groundtruth scores. This phenomenon indicates that our MHSCNet captures the meaningful short-range and long-range temporal dependency via the hierarchical ShotConv network.

4.3 Ablation Study

We conduct a series of experiments on the SumMe [6] dataset and the TVSum [44] datasets to better understand the proposed model and verify the contribution of each component.

Multi Modality. We first study the influence from the additional modality information of our MHSCNet. Without the audio modality and the caption modality, our model also achieve the best result on the SumMe benchmark and the TVSum benchmark compared to the state-of-the-art methods. As observed in Table 1, the second-best method equipped with the same backbone network(GoogLeNet) achieve 51.6 % on the SumMe dataset and 64.2% on the TVSum dataset. The results are shown in Table 4. With the help of the local information via the audio modality, the model achieves 2.5% and 0.2% gain on two benchmarks, respectively. Similarly, the caption modality provides complementary global information which

Table 1: Comparisons of F -Score (%) and parameters (in million) with peer supervised techniques on SumMe [6] and TVSum [44], with various data configurations including standard data, augmented data, and transfer data settings. The scores in bold indicate the best values. “-” denotes that the results are not available. Bimodal approaches are marked with \diamond . For some unsupervised learning methods, we report their results in a supervised manner. As CLIP-It, we report their results with two different backbone networks. For fair comparisons with previous methods, we mainly adopt GoogLeNet features.

Method	Backbone	SumMe			TVSum			Params
		Standard	Augment	Transfer	Standard	Augment	Transfer	
Random summary [29]	-	41.0	-	-	57.0	-	-	0.0
SUM-GAN [26]	GoogLeNet [46]	41.7	43.6	-	56.3	61.2	-	295.9
SUM-FCN [42]	GoogLeNet [46]	47.5	51.1	44.1	56.8	59.2	58.2	116.5
SUM-DeepLab [42]	GoogLeNet [46]	48.8	50.2	45.0	58.4	59.8	58.9	-
DR-DSN [57]	GoogLeNet [46]	42.1	43.9	42.6	58.1	59.8	58.9	2.6
ACGAN [8]	GoogLeNet [46]	47.2	-	-	59.4	-	-	-
\diamond DQSN [58]	GoogLeNet [46]	-	-	-	58.6	-	-	-
\diamond DSSE [49]	AlexNet [19]	-	-	-	57.0	-	-	-
\diamond AVRN [54]	GoogLeNet [46]	44.1	44.9	43.2	59.7	60.5	58.7	-
VASNet [4]	GoogLeNet [46]	49.7	51.1	-	61.4	62.4	-	7.4
DSNet-AB [59]	GoogLeNet [46]	50.2	50.7	46.5	62.1	63.9	59.4	8.5
DSNet-AF [59]	GoogLeNet [46]	51.2	53.3	47.6	61.9	62.2	58.0	4.3
MC-VSA [24]	GoogLeNet [46]	51.6	53.0	48.1	63.7	64.0	59.5	-
SumGraph [36]	GoogLeNet [46]	51.4	52.9	48.7	63.9	65.8	60.5	5.5
\diamond CLIP – It* [27]	GoogLeNet [46]	51.6	53.5	49.4	64.2	66.3	61.3	-
\diamond CLIP – It [27]	CLIP-ViT-B/32 [40]	54.2	56.4	51.9	66.3	69.0	65.5	-
MHSCNet (ours)	GoogLeNet [46]	55.3	56.9	49.8	69.3	69.4	61.0	134.6

Table 2: The diversity scores of generated summaries on the SumMe[6] and TVSum [44] datasets.

Method	Backbone	SumMe	TVSum
dppLSTM [52]	GoogLeNet [46]	0.591	0.463
DR-DSN [57]	GoogLeNet [46]	0.594	0.464
DSNet-AF [59]	GoogLeNet [46]	0.642	0.476
DSNet-AB [59]	GoogLeNet [46]	0.664	0.477
MHSCNet (ours)	GoogLeNet [46]	0.732	0.530

Table 3: Kendall’s τ [15] and Spearman’s ρ [60] correlation coefficients computed on the TVSum benchmark [44].

Method	Backbone	Kendall’s τ	Spearman’s ρ
Random summary [29]	GoogLeNet [46]	0.000	0.000
dppLSTM [52]	GoogLeNet [46]	0.042	0.055
DR-DSN [57]	GoogLeNet [46]	0.020	0.026
HSA-RNN [55]	VGG16 [43]	0.082	0.088
SumGraph [36]	GoogLeNet [46]	0.094	0.138
MC-VSA [24]	GoogLeNet [46]	0.116	0.142
AVRN [54]	GoogLeNet [46]	0.096	0.104
DASN [5]	GoogLeNet [46]	0.058	0.065
CLIP – It [27]	CLIP-ViT-B/32 [40]	0.108	0.147
Human [29]	-	0.177	0.204
MHSCNet (ours)	GoogLeNet [46]	0.154	0.225

enhances the performance by 1.8% and 0.3% for our model. Furthermore, our model combining the audio modality and the caption modality can achieve a higher F -score.

Hierarchical ShotConv Network. Then, we study the influence at different scales of the shots in the hierarchical ShotConv network and show the results in Table 5. Compared to the double-scale ShotConv networks, the single scale ShotConv networks perform worse. However, the network with the single middle-scale shot convolution still achieves the competitive performance on the SumMe dataset and the TVSum dataset due to the split shot length being matched with the initial shot length of the video. Similarly, the

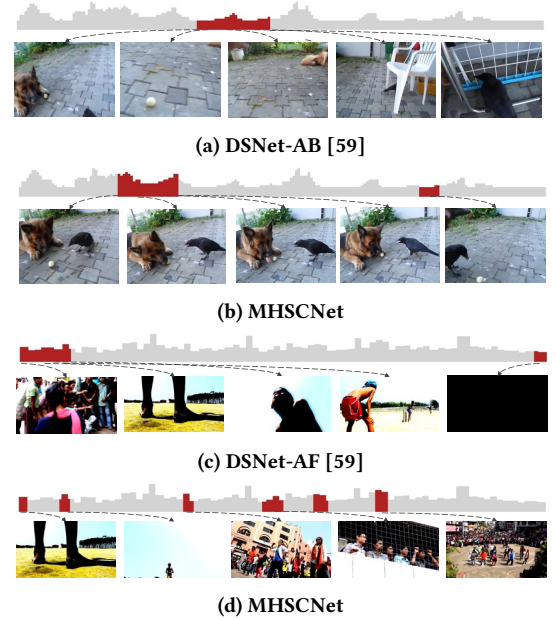


Figure 5: Qualitative results on the SumMe benchmark [6] and the TVSum benchmark [44]: (a) DSNet-AF [59], (b) MHSCNet for video number 25 on the SumMe benchmark, (c) DSNet-AF [59], (d) MHSCNet for video number 34 on the TVSum benchmark. The ground-truth importance scores are shown as gray background and the selected subset shots are shown as red background. Five selected frames are randomly shown for the summary results.

network with a single long scale shot convolution obtains a 67.6% F -score which is slightly lower than the best results of the double scale networks. Moreover, we observe that a double scale network

Table 4: Ablation study for various information of the modality in MHSCNet with F-score evaluation metric on the SumMe [6] benchmark and the TVSum [44] benchmark.

Modality	SumMe	TVSum
Image	52.0	68.0
Image+Audio	54.5	68.2
Image+Caption	53.8	68.3
Ours (Image+Audio+Caption)	55.3	69.3

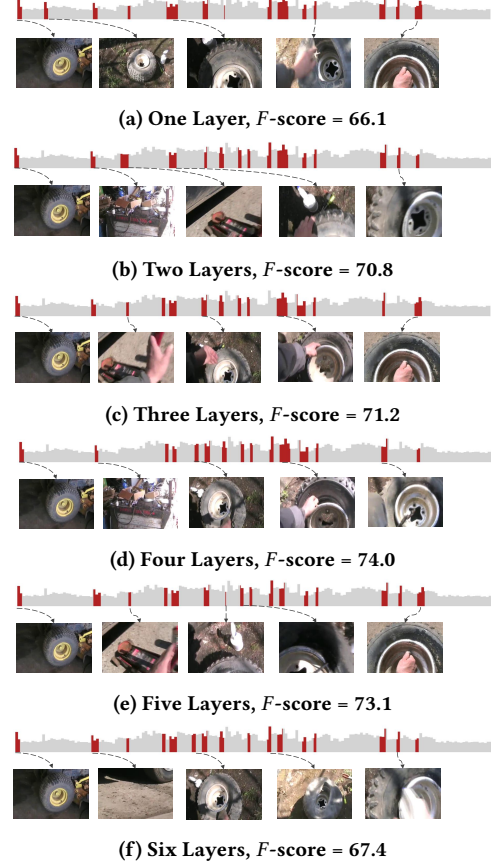
such as M+S drops the performance compared to a single scale network such as M. The negative transfer occasionally happen in the double scale network. However, our MHSCNet equipped with three scales can achieve the best results due to the strong adaptivity to the video length.

Table 5: Ablation study on our hierarchical ShotConv network with F-score metric on SumMe[6] and TVSum [44] benchmarks. L, M and S means long-scale, middle-scale and short-scale ShotConv module, respectively.

Scale	SumMe	TVSum
L	52.2	67.6
M	54.1	67.2
S	52.1	65.4
L+M	54.4	67.5
L+S	53.0	66.0
M+S	53.6	67.7
Ours (L+M+S)	55.3	69.3

The Layers Number. Besides, we provide a ablation study for the layers number of the hierarchical ShotConv network. Benefitting from the cross-shot padding and the stacked hierarchical ShotConv network, the global information will propagate within the shot implicitly as mentioned in main text Sec. 3.4.3. The quantitative comparison can be found in Table 6. Note that the results with respect to number of layer 1 represent the results without any global information propagation inner the shot. We observe that the deeper hierarchical ShotConv networks (1 \rightarrow 4) achieve the better performance. When the number of layers is 4, the global information from all shots can be passed within one shot. Due to the overfitting problem, the deeper hierarchical ShotConv networks (4 \rightarrow 6) lead to the worse results. In addition, we also show the qualitative results corresponding to the number of hierarchical ShotConv networks in Fig. 6. In each illustrated summary, we visualize 5 sampled frames from the highlighted predicted frames.

Cross-shot Padding Ratio. Last, we study the cross-shot padding ratio for the hierarchical ShotConv network. With a larger padding ratio (0 \rightarrow 0.05), the performance of the F-score on the two benchmarks raises accordingly. When the larger padding ratio is considered (0.05 \rightarrow 0.09), the performance drop accordingly. We think the reason is that the larger padding ratio reduces the weight of the initial frame within the shot. We also observe that the network without the cross-shot padding achieve the worst results because of the lack of the global information propagation.

**Figure 6: Qualitative results on the the TVSum benchmark [44]: (a) - (f) : one - six layers which represent the stacked hierarchical ShotConv network for video number 1 on the TVSum benchmark. The ground-truth importance scores are shown as gray background and the selected subset shots are shown as red background. Five selected frames are randomly shown for the summary results.****Table 6: Ablation study for the layers number L of the hierarchical ShotConv network with F-score (%) evaluation metric, parameters (M) and runtime (ms).**

L	SumMe	TVSum	Params	Runtime
1	50.8	66.1	33.8	6.6
2	51.9	67.1	67.4	12.1
3	52.3	68.2	101.0	17.7
5	53.5	68.5	168.2	32.8
6	51.8	67.9	201.7	36.3
4	55.3	69.3	134.6	23.7

5 CONCLUSION

In this paper, we propose a novel multimodal framework with a hierarchical ShotConv network for video summarization. Unlike existing unimodal or bimodal methods which only adopt visual cues with one additional modal information to construct the frame representation, our MHSCNet exploits the caption and the audio

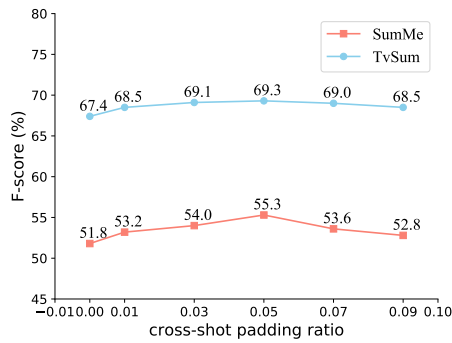


Figure 7: Ablation study of the cross-shot padding ratio on the SumMe[6] benchmark and the TVSum [44] benchmark.

modality to enhance the frame-wise representation and explore the semantic relations. To evaluate the frame-level importance score in a fair and comprehensive manner, we further propose a hierarchical ShotConv network with the cross-shot padding mechanism to model the frame-to-frame interaction both within and across the shot. The hierarchical ShotConv network generates an adaptive shot-aware representation that captures the short-range temporal dependency explicitly and long-range temporal dependency implicitly. Extensive experimental results on multiple datasets with comprehensive evaluation criteria demonstrate the superiority of our approach over most existing state-of-the-art methods.

REFERENCES

- [1] Sijia Cai, Wangmeng Zuo, Larry S Davis, and Lei Zhang. 2018. Weakly-supervised video summarization using variational encoder-decoder and web prior. In *Proceedings of the European conference on computer vision (ECCV)*. 184–200.
- [2] Wen-Sheng Chu, Yale Song, and Alejandro Jaimes. 2015. Video co-summarization: Video summarization by visual co-occurrence. In *Proceedings of the IEEE conference on computer vision and pattern recognition*. 3584–3592.
- [3] Sandra Eliza Fontes De Avila, Ana Paula Brandao Lopes, Antonio da Luz Jr, and Arnaldo de Albuquerque Araújo. 2011. VSUMM: A mechanism designed to produce static video summaries and a novel evaluation method. *Pattern Recognition Letters* 32, 1 (2011), 56–68.
- [4] Jiri Fajtl, Hajar Sadeghi Sokeh, Vasileios Argyriou, Dorothy Monekso, and Paolo Remagnino. 2018. Summarizing videos with attention. In *Asian Conference on Computer Vision*. Springer, 39–54.
- [5] Hao Fu, Hongxing Wang, and Jianyu Yang. 2021. Video Summarization with a Dual Attention Capsule Network. In *2020 25th International Conference on Pattern Recognition (ICPR)*. IEEE, 446–451.
- [6] Michael Gygli, Helmut Grabner, Hayko Riemenschneider, and Luc Van Gool. 2014. Creating summaries from user videos. In *European conference on computer vision*. Springer, 505–520.
- [7] Michael Gygli, Helmut Grabner, and Luc Van Gool. 2015. Video summarization by learning submodular mixtures of objectives. In *Proceedings of the IEEE conference on computer vision and pattern recognition*. 3090–3098.
- [8] Xufeng He, Yang Hua, Tao Song, Zongpu Zhang, Zhengui Xue, Ruhui Ma, Neil Robertson, and Haibing Guan. 2019. Unsupervised video summarization with attentive conditional generative adversarial networks. In *Proceedings of the 27th ACM International Conference on Multimedia*. 2296–2304.
- [9] Shawn Hershey, Sourish Chaudhuri, Daniel PW Ellis, Jort F Gemmeke, Aren Jansen, R Channing Moore, Manoj Plakal, Devin Platt, Rif A Saurous, Bryan Seybold, et al. 2017. CNN architectures for large-scale audio classification. In *2017 IEEE international conference on acoustics, speech and signal processing (icassp)*. IEEE, 131–135.
- [10] Jia-Hong Huang, Luka Murn, Marta Mrak, and Marcel Worring. 2021. GPT2MVS: Generative Pre-trained Transformer-2 for Multi-modal Video Summarization. *arXiv preprint arXiv:2104.12465* (2021).
- [11] Vladimir Iashin and Esa Rahtu. 2020. A better use of audio-visual cues: Dense video captioning with bi-modal transformer. *arXiv preprint arXiv:2005.08271* (2020).
- [12] Neel Joshi, Wolf Kienzle, Mike Toelle, Matt Uyttendaele, and Michael F Cohen. 2015. Real-time hyperlapse creation via optimal frame selection. *ACM Transactions on Graphics (TOG)* 34, 4 (2015), 1–9.
- [13] Yunjae Jung, Donghyeon Cho, Dahun Kim, Sanghyun Woo, and In So Kweon. 2019. Discriminative feature learning for unsupervised video summarization. In *Proceedings of the AAAI Conference on Artificial Intelligence*, Vol. 33. 8537–8544.
- [14] Hong-Wen Kang, Yasuyuki Matsushita, Xiaoou Tang, and Xue-Quan Chen. 2006. Space-time video montage. In *2006 IEEE Computer Society Conference on Computer Vision and Pattern Recognition (CVPR'06)*, Vol. 2. IEEE, 1331–1338.
- [15] Maurice G Kendall. 1945. The treatment of ties in ranking problems. *Biometrika* 33, 3 (1945), 239–251.
- [16] Aditya Khosla, Raffay Hamid, Chih-Jen Lin, and Neel Sundaresan. 2013. Large-scale video summarization using web-image priors. In *Proceedings of the IEEE conference on computer vision and pattern recognition*. 2698–2705.
- [17] Gunhee Kim and Eric P Xing. 2014. Reconstructing storyline graphs for image recommendation from web community photos. In *Proceedings of the IEEE Conference on Computer Vision and Pattern Recognition*. 3882–3889.
- [18] Johannes Kopf, Michael F Cohen, and Richard Szeliski. 2014. First-person hyperlapse videos. *ACM Transactions on Graphics (TOG)* 33, 4 (2014), 1–10.
- [19] Alex Krizhevsky, Ilya Sutskever, and Geoffrey E Hinton. 2012. Imagenet classification with deep convolutional neural networks. *Advances in neural information processing systems* 25 (2012).
- [20] Yong Jae Lee, Joydeep Ghosh, and Kristen Grauman. 2012. Discovering important people and objects for egocentric video summarization. In *2012 IEEE conference on computer vision and pattern recognition*. IEEE, 1346–1353.
- [21] Jindrich Libovický, Shruti Palaskar, Spandana Gella, and Florian Metze. 2018. Multimodal abstractive summarization of open-domain videos. In *Proceedings of the Workshop on Visually Grounded Interaction and Language (ViGIL)*. NIPS.
- [22] Tsung-Yi Lin, Priya Goyal, Ross Girshick, Kaiming He, and Piotr Dollár. 2017. Focal loss for dense object detection. In *Proceedings of the IEEE international conference on computer vision*. 2980–2988.
- [23] David Liu, Gang Hua, and Tsuhan Chen. 2010. A hierarchical visual model for video object summarization. *IEEE transactions on pattern analysis and machine intelligence* 32, 12 (2010), 2178–2190.
- [24] Yen-Ting Liu, Yu-Jhe Li, and Yu-Chiang Frank Wang. 2020. Transforming multi-concept attention into video summarization. In *Proceedings of the Asian Conference on Computer Vision*.
- [25] Zheng Lu and Kristen Grauman. 2013. Story-driven summarization for egocentric video. In *Proceedings of the IEEE Conference on Computer Vision and Pattern Recognition*. 2714–2721.
- [26] Behrooz Mahasseni, Michael Lam, and Sinisa Todorovic. 2017. Unsupervised video summarization with adversarial lstm networks. In *Proceedings of the IEEE conference on Computer Vision and Pattern Recognition*. 202–211.
- [27] Medhini Narasimhan, Anna Rohrbach, and Trevor Darrell. 2021. CLIP-It! language-guided video summarization. In *NeurIPS*, Vol. 34.
- [28] Chong-Wah Ngo, Yu-Fei Ma, and Hong-Jiang Zhang. 2003. Automatic video summarization by graph modeling. In *Proceedings Ninth IEEE International Conference on Computer Vision*. IEEE, 104–109.
- [29] Mayu Otani, Yuta Nakashima, Esa Rahtu, and Janne Heikkilä. 2019. Rethinking the evaluation of video summaries. In *Proceedings of the IEEE/CVF Conference on Computer Vision and Pattern Recognition*. 7596–7604.
- [30] Mayu Otani, Yuta Nakashima, Esa Rahtu, Janne Heikkilä, and Naokazu Yokoya. 2016. Video summarization using deep semantic features. In *Asian Conference on Computer Vision*. Springer, 361–377.
- [31] Shruti Palaskar, Jindrich Libovický, Spandana Gella, and Florian Metze. 2019. Multimodal abstractive summarization for how2 videos. *arXiv preprint arXiv:1906.07901* (2019).
- [32] Rameswar Panda, Abir Das, Ziyang Wu, Jan Ernst, and Amit K Roy-Chowdhury. 2017. Weakly supervised summarization of web videos. In *Proceedings of the IEEE International Conference on Computer Vision*. 3657–3666.
- [33] Rameswar Panda, Niluthpol Chowdhury Mithun, and Amit K Roy-Chowdhury. 2017. Diversity-aware multi-video summarization. *IEEE Transactions on Image Processing* 26, 10 (2017), 4712–4724.
- [34] Rameswar Panda and Amit K Roy-Chowdhury. 2017. Collaborative summarization of topic-related videos. In *Proceedings of the IEEE Conference on Computer Vision and Pattern Recognition*. 7083–7092.
- [35] Rameswar Panda and Amit K Roy-Chowdhury. 2017. Multi-view surveillance video summarization via joint embedding and sparse optimization. *IEEE Transactions on Multimedia* 19, 9 (2017), 2010–2021.
- [36] Jungin Park, Jiyoung Lee, Ig-Jae Kim, and Kwanghoon Sohn. 2020. Sumgraph: Video summarization via recursive graph modeling. In *ECCV*. Springer, 647–663.
- [37] Yair Poleg, Tavi Halperin, Chetan Arora, and Shmuel Peleg. 2015. Egosampling: Fast-forward and stereo for egocentric videos. In *Proceedings of the IEEE Conference on Computer Vision and Pattern Recognition*. 4768–4776.
- [38] Danila Potapov, Matthijs Douze, Zaid Harchaoui, and Cordelia Schmid. 2014. Category-specific video summarization. In *European conference on computer vision*. Springer, 540–555.

- [39] Yael Pritch, Alex Rav-Acha, Avital Gutman, and Shmuel Peleg. 2007. Webcam synopsis: Peeking around the world. In *2007 IEEE 11th International Conference on Computer Vision*. IEEE, 1–8.
- [40] Alec Radford, Jong Wook Kim, Chris Hallacy, Aditya Ramesh, Gabriel Goh, Sandhini Agarwal, Girish Sastry, Amanda Askell, Pamela Mishkin, Jack Clark, et al. 2021. Learning transferable visual models from natural language supervision. *arXiv preprint arXiv:2103.00020* (2021).
- [41] Mrigank Rochan and Yang Wang. 2019. Video summarization by learning from unpaired data. In *Proceedings of the IEEE/CVF Conference on Computer Vision and Pattern Recognition*. 7902–7911.
- [42] Mrigank Rochan, Linwei Ye, and Yang Wang. 2018. Video summarization using fully convolutional sequence networks. In *Proceedings of the European Conference on Computer Vision (ECCV)*. 347–363.
- [43] Karen Simonyan and Andrew Zisserman. 2014. Very deep convolutional networks for large-scale image recognition. *arXiv preprint arXiv:1409.1556* (2014).
- [44] Yale Song, Jordi Vallmitjana, Amanda Stent, and Alejandro Jaimes. 2015. Tvsum: Summarizing web videos using titles. In *Proceedings of the IEEE conference on computer vision and pattern recognition*. 5179–5187.
- [45] Min Sun, Ali Farhadi, Ben Taskar, and Steve Seitz. 2014. Salient montages from unconstrained videos. In *European Conference on Computer Vision*. Springer, 472–488.
- [46] Christian Szegedy, Wei Liu, Yangqing Jia, Pierre Sermanet, Scott Reed, Dragomir Anguelov, Dumitru Erhan, Vincent Vanhoucke, and Andrew Rabinovich. 2015. Going deeper with convolutions. In *Proceedings of the IEEE conference on computer vision and pattern recognition*. 1–9.
- [47] Fisher Yu and Vladlen Koltun. 2015. Multi-scale context aggregation by dilated convolutions. *arXiv preprint arXiv:1511.07122* (2015).
- [48] Li Yuan, Francis EH Tay, Ping Li, Li Zhou, and Jiashi Feng. 2019. Cycle-sum: cycle-consistent adversarial lstm networks for unsupervised video summarization. In *Proceedings of the AAAI Conference on Artificial Intelligence*, Vol. 33. 9143–9150.
- [49] Yitian Yuan, Tao Mei, Peng Cui, and Wenwu Zhu. 2017. Video summarization by learning deep side semantic embedding. *IEEE Transactions on Circuits and Systems for Video Technology* 29, 1 (2017), 226–237.
- [50] Kuo-Hao Zeng, Tseng-Hung Chen, Juan Carlos Niebles, and Min Sun. 2016. Generation for user generated videos. In *European conference on computer vision*. Springer, 609–625.
- [51] Ke Zhang, Wei-Lun Chao, Fei Sha, and Kristen Grauman. 2016. Summary transfer: Exemplar-based subset selection for video summarization. In *Proceedings of the IEEE conference on computer vision and pattern recognition*. 1059–1067.
- [52] Ke Zhang, Wei-Lun Chao, Fei Sha, and Kristen Grauman. 2016. Video summarization with long short-term memory. In *European conference on computer vision*. Springer, 766–782.
- [53] Ke Zhang, Kristen Grauman, and Fei Sha. 2018. Retrospective encoders for video summarization. In *Proceedings of the European Conference on Computer Vision (ECCV)*. 383–399.
- [54] Bin Zhao, Maoguo Gong, and Xuelong Li. 2021. AudioVisual Video Summarization. *arXiv preprint arXiv:2105.07667* (2021).
- [55] Bin Zhao, Xuelong Li, and Xiaoqiang Lu. 2018. Hsa-rnn: Hierarchical structure-adaptive rnn for video summarization. In *Proceedings of the IEEE conference on computer vision and pattern recognition*. 7405–7414.
- [56] Kaiyang Zhou, Yu Qiao, and Tao Xiang. 2017. Deep Reinforcement Learning for Unsupervised Video Summarization with Diversity-Representativeness Reward. *arXiv:1801.00054* (2017).
- [57] Kaiyang Zhou, Yu Qiao, and Tao Xiang. 2018. Deep reinforcement learning for unsupervised video summarization with diversity-representativeness reward. In *Proceedings of the AAAI Conference on Artificial Intelligence*, Vol. 32.
- [58] Kaiyang Zhou, Tao Xiang, and Andrea Cavallaro. 2018. Video summarisation by classification with deep reinforcement learning. *arXiv preprint arXiv:1807.03089* (2018).
- [59] Wencheng Zhu, Jiwen Lu, Jiahao Li, and Jie Zhou. 2020. DSNet: A Flexible Detect-to-Summarize Network for Video Summarization. *IEEE Transactions on Image Processing* 30 (2020), 948–962.
- [60] Daniel Zwillinger and Stephen Kokoska. 1999. *CRC standard probability and statistics tables and formulae*. Crc Press.